DISCLAIMER NOTICE

THIS DOCUMENT IS BEST QUALITY PRACTICABLE. THE COPY FURNISHED TO DTIC CONTAINED A SIGNIFICANT NUMBER OF PAGES WHICH DO NOT REPRODUCE LEGIBLY.

TECHNICAL MANUSCRIPT 98

THE CALIBRATION OF A MODIFIED ANDERSEN BACTERIAL AEROSOL SAMPLER

OCTOBER 1963

UNITED STATES ARMY
BIOLOGICAL LABORATORIES
FORT DETRICK

U.S. ARMY BIOLOGICAL LABORATORIES
Fort Detrick, Frederick, Maryland

TECHNICAL MANUSCRIPT 98

THE CALIBRATION OF A MODIFIED ANDERSEN BACTERIAL AEROSOL SAMPLER

Kenneth R. May

(Microbiological Research Establishment,
Porton, Wiltshire, England)

Physical Defense Division
DIRECTOR OF MEDICAL RESEARCH

October 1963

This work was performed by Mr. May during a one-year temporary assignment to the U. S. Army Biological Laboratories from the Microbiological Research Establishment, Porton, England, which provided all funding.

UNITED STATES ARMY BIOLOGICAL LABORATORIES
FORT DETRICK, FREDERICK, MARYLAND

Erratum

To: Recipients of Technical Manuscript 98
From: Chief, Editorial Branch, Technical Information Division

The listing of the Division and the Directorate on page 1 of Technical Manuscript 98 is in error. Please substitute the following:

Physical Sciences Division
DIRECTOR OF BIOLOGICAL RESEARCH

ACKNOWLEDGMENT

It is a pleasure to thank Mr. C. O. Swenson for making many experimental models with great skill, Lt. W. N. Mott for much of the microscopical work, and many other members of the Physical Sciences Division, Fort Detrick, for expert assistance.

ABSTRACT

A study of the flow regime in the commercial Andersen Sampler revealed defects in the sampling of the larger air-borne particles. Satisfactory sampling was obtained by redesigning the hole pattern of the top stages and adding one more stage to extend the range of the instrument. A new, rational, hole pattern is suggested for the lower stages. With both patterns a special colony-counting mask can be used to facilitate the assay. A calibration of the modified system is presented that enables particle size distribution curves to be drawn from the colony counts.

CONTENTS

TABLES

FIGURES

I. INTRODUCTION

The Andersen Sampler[1] collects six size-graded aerosol fractions in Petri dishes by a system of multi-jet cascade impaction. It has found wide acceptance for sampling viable aerosols when it is desired to estimate the numbers and sizes of the actual air-borne particles, rather than to estimate the total number of viable cells in those particles, as one obtains, for example, from liquid impingers.

In attempting to obtain a calibration for the commercial sampler, Model 0101, so that size distribution curves could be drawn from the colony counts, I found irregularities in the deposition of the larger particles that made a valid calibration impracticable. The intake efficiency for the larger particles was also poor. This paper presents a study of these faults and their origin, from the results of which a modified design was developed. A calibration of this design enables particle size distribution curves and total mass to be obtained from the colony counts.

In justification for the improvement to the large-particle (diameter greater than five microns) efficiency of this sampler, it is pointed out that in this category fall many of the infective particles generated by such processes as blanket shaking, sweeping, talking, coughing, and sneezing. Also, a high proportion of the mass of sprayed aerosols usually lies in the larger particles.

II. MATERIALS AND METHODS

A. PRELIMINARY STUDIES

To study the impaction characteristics of each stage, glass discs were set up in special Petri dishes at exactly the same height as is the agar with the standard fill of 27 milliliters. This setting is very important because the clearance between the underside of the sieve plate (S in Figure 1) and the collection surface affects the airflow. Andersen[1] gives this clearance as 0.1 inch but our measurements with fresh agar gave a mean of 0.07 inch which can vary a little with the dish used, the age of the agar, and the position of the sampler. The average thickness of agar is 0.175 inch.

Heavy samples of droplets or solid particles were then taken. If all jets of a stage have equal impaction efficiency, the aggregates of thousands of particles under each jet would give visible spots of uniform density. This was found to be quite untrue for Stages 1 and 2 (for particles greater than five microns). Samples of viable particles of sprayed Serratia marcescens were also taken to study the effects on them of unequal impact efficiency over a stage.

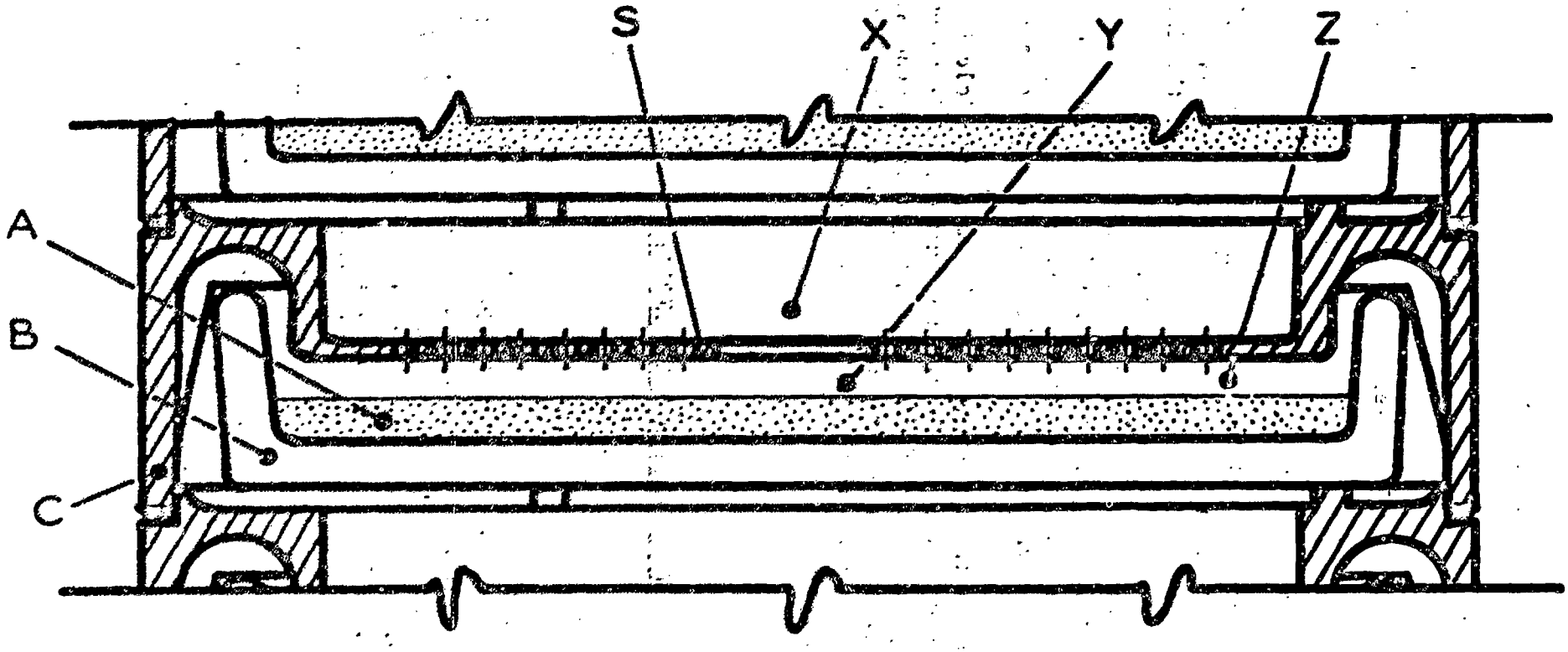

Figure 1. Vertical Section Through an Andersen Stage. A, agar in Petri dish B. C, metal body, integral with sieve plate S, drilled with 400 holes, decreasing in size from stage to stage.

B. MODIFIED SAMPLER

Uniform efficiency over a stage was obtained by a complete redesign of the jet hole pattern and jet-to-agar clearance. It was strongly desired to extend the useful range of the sampler to particles larger than 12 microns. This was done by adding a top stage of the same new design, after tests with other geometry including a single-jet stage.

C. INTAKE EFFICIENCY AND INTERNAL LOSSES

Studies were made of the efficiency of collection of particles as large as 30 microns, by taking samples, in a large chamber, of dyed, involatile and uniform droplets generated by a spinning-top sprayer. Colorimetric estimations were made of the dye washed from the glass discs and from other parts of the sampler. It has not been possible, to date, to study the important question of intake efficiency in wind-borne aerosols.

D. CALIBRATION

An excellent recent review of the calibration of cascade impactors has been given by Mercer.[2] He prefers the use of the "50 per cent cut-off" diameter (d_{50}) as a stage characteristic rather than the mass median diameter (MMD). At a standard sampling rate, the former cannot vary, whereas it is possible for the MMD to show some variation with atypical aerosol distributions. Further discussion of this subject is redundant here, Mercer's paper being recommended reading. In the present work, calibrations of both d_{50} and MMD were obtained.

Calibration was done by detailed fluorescent microscope counting and sizing of bacterial aerosol particles of suitable concentration on sticky glass discs in lieu of the agar. The eyepiece graticule described by May[3] was used in this work and two observers gave very consistent results. At least 300 particles were sized per stage in each experiment, and enough impact areas were completely scanned to give a count of at least 3000 particles per stage and thus a reliable estimate of the total stage numbers.

Pneumatic spraying of suspensions of B. aerogenes, at a concentration of 2×10^{11} organisms per milliliter produced the test particles. The suspensions had been heat-sterilized, stained with primuline dye, centrifuged and resuspended in clean water. The resulting particles after evaporation of the water are inert, strongly fluorescent under ultraviolet light, and are spherical except for the smallest particles, which consist of single, or very few, cells and have a density of 1.37 grams per cubic centimeter. This is similar to the density of most other bacterial particles. Almost any other bacterial suspension could have been used and the addition of, say, 0.1 per cent of sodium fluorescein would give adequate fluorescence. The advantage of the fluorescence is that it renders the particles very easy to see and eliminates any possibility of confusion with atmospheric dust at the smallest sizes.

It was decided to use bacterial particles because of their realism and ease of production, and after consideration of many other possibilities. In particular, wax spheres made by spraying hot molten wax, widely used in similar work (e.g., Andersen[1]), were rejected after attempt to measure their density by flotation in liquid mixtures adjusted to the same density. It was found that they had a very wide range of density because of included air bubbles of extremely variable size. Also, doublet spheres were common.

From the size counts of each stage, the best fit cumulative number distribution curves were plotted on logarithmic-probability paper. In general, these curves gave very good straight lines over most of their length. From these curves, divided into size ranges half as wide as those given by the eyepiece graticule, smoothed frequency histograms of absolute numbers of particles sampled per size range were drawn for each stage. The intersections of these are the d_{50} values. Very good reproducibility from test to test was obtained. The same curves also yielded the characteristic cut-off curves for each stage (Figure 2). MMD's were obtained from conventional plots of the cumulative volume on log probability paper. The final required parameter, the mean volume diameter (MVD) for each stage, is $(\Sigma\, n\, d^3 / \Sigma\, n)^{1/3}$ where there are n particles in each range of mean diameter d.

III. RESULTS

Figure 3 is a photograph of a heavy sample of dyed droplets on the first three Andersen stages. The maximum drop diameter was 12 microns. Note that there are severe density variations over the Stage 1 discs, both with and without the intake cone, and on Stage 2. On Stage 3 it is just detectable in the original that the spots slightly increase in density from inside outwards. Stages 4, 5, and 6 are not shown because they appear quite uniform.

To explain and eliminate these variations, the internal air flow regime must be understood. In Figure 1, X is the whole zone above S, Y the zone under the center of S, and Z the annular zone under the outer holes of S. P_x, P_y, and P_z will signify the static pressures in zones X, Y, and Z. These static pressures were measured with a micromanometer and Table I was obtained. The spot-density variations arise from interactions of the factors (a) radial pressure fall, (b) pattern interference, (c) particle size, and (d) the intake cone. These will be considered individually.

(a) Radial pressure fall. The radial pressure fall (rpf) (Table I, Column 2) is explained by Bernoulli's theorem from the fact that there is no flow in zone Y, while the full flow of 1 cubic foot per minute has built up through zone Z. Column 2 shows that there is only a slight increase in rpf from stage to stage. This is to be expected because the geometry is constant,

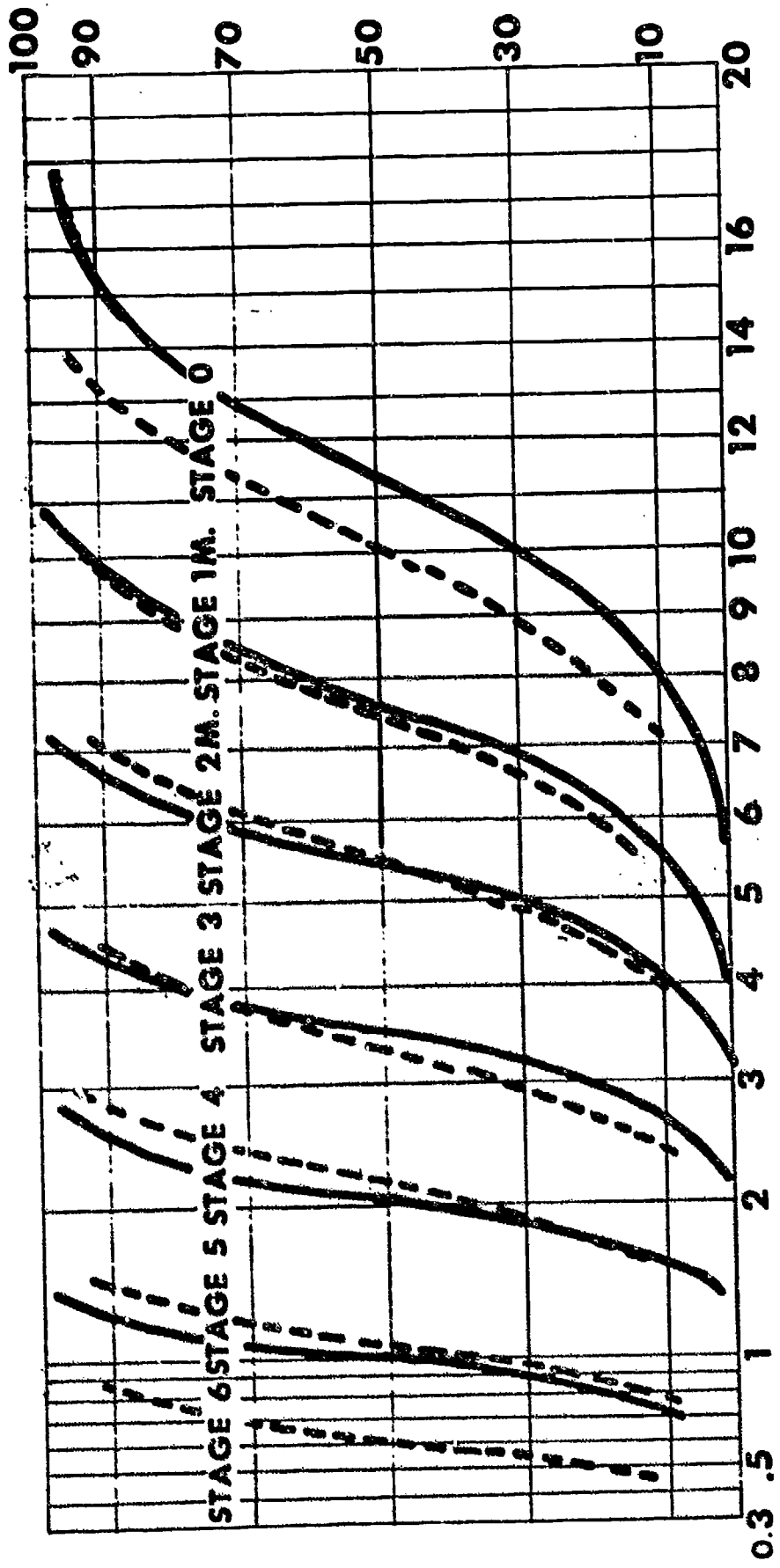

Figure 2. Stage Cut-Off Curves for Modified Andersen Sampler. Stages 3, 4, 5, and 6 unmodified. Continuous curves, present calibration. Dashed curves calculated from Ranz and Wong.

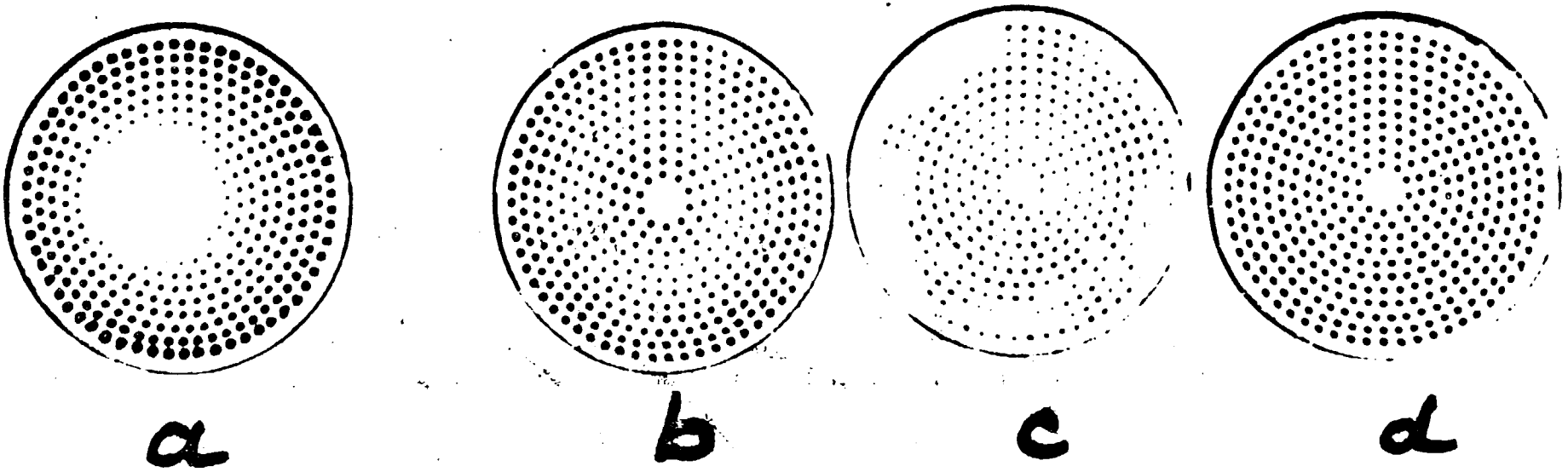

Figure 3. Heavy Sample of Dyed Droplets in Standard Andersen Sampler. a, Stage 1 without cone; b, stage 1 with cone; c, stage 2; d, stage 3.

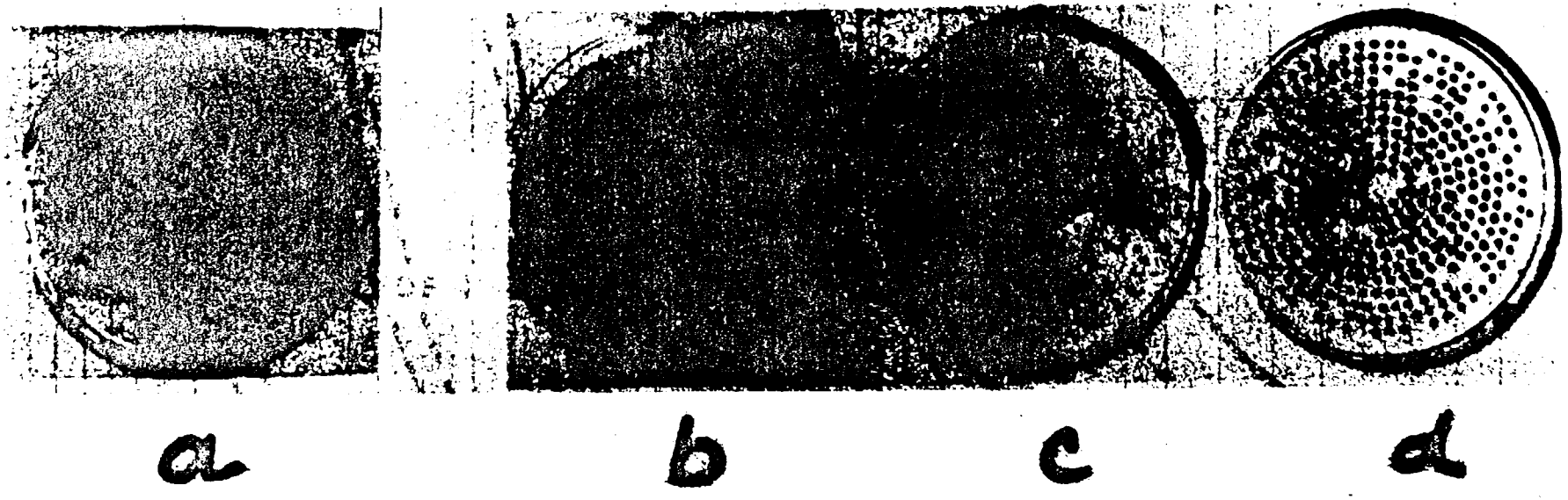

Figure 4. Colonies of S. marcescens from Standard Andersen Sampler. a, b, c, and d as for Figure 3.

TABLE I. INTERNAL STATIC PRESSURE DIFFERENCES[a/] IN STANDARD ANDERSEN SAMPLER

Stage	Radial Pressure Fall, P_y-P_z	Pressure Fall Across Outer and Inner Jets, P_x-P_z	P_x-P_y	Ratio of Outer and Inner Jet Velocities, $(P_x-P_z/P_x-P_y)^{\frac{1}{2}}$
1	0.26	0.34	0.08	2.05
2	0.33	0.76	0.43	1.33
3	0.42	1.66	1.26	1.15
4	0.45	6.2	5.7	1.05
5	0.51	33.5	33.0	1.01
6	0.63	81.5	80.9	1.004

a. In millimeters of water.

but the more violent interjet turbulence as jet speeds increase gives slowly increasing outflow resistance to the spent air. Columns 3 and 4 show rapid increases down the stages as the holes decrease in size. Column 5, the square root of the ratio of Column 3 to Column 4, gives the ratio of the velocities through the outer and inner jets. In the lower stages, the rpf is relatively negligible, so that velocity differences between the outer and inner holes are too small to have a significant effect on the impaction efficiency. But in the upper stages, where rpf is comparable to jet pressure fall, jet velocity differences up to a factor of 2 exist in Stage 1 (Column 5). Here, then, we have twice as many particles going through the outer holes as through the inner ones, and at higher impaction efficiencies. If the predominant particle size happens to be on the steep part of the cut-off curve (see Figure 2), enormous differences between inner and outer impaction can result, as in Figure 3 (a) where the inner spots are invisible and the spot density increases steadily outwards as the jet velocity increases. Similar effects occur on Stage 2, Figure 3 (c), out to the seventh ring of holes from the center, but less obviously because the rpf is relatively smaller than in Stage 1. Beyond the seventh ring of holes, pattern interference effects dominate.

(b) Pattern interference. The hole pattern chosen by Andersen has no symmetry but does have the same groupings of holes in all stages. In Figures 3 and 4 the discs and dishes are orientated so that the pattern is in the same position in each case. In Figure 3 (c) the deposit spots in the three or four outer rings are prominent at 12 o'clock, 2, 4:30, 7:30, and 10 o'clock, while in the intermediate regions they are very faint or absent. This is because in the heavier outer zones the holes happen to be arranged in parallel radial "streets" so that jets can impact their particle burden in a region protected from the force of the outflowing air by their upstream neighbors. Between the street zones, holes merge into a diamond pattern where, in the top two stages, the unprotected air jets, which are relatively broad and feeble, are readily blown aside. In the lower stages, jets are thin and of higher energy and cannot be mastered by the outflow of spent air. Pattern interference effects are often very prominent in Stage 1, more so than in the particular example of Figure 3 (b). In Figure 3 (c), jets are not blown aside until after the eighth or ninth rings of holes from the center because the outflow of spent air is inadequate before that zone. When jets are blown aside to any extent at all, microscopic examination of the deposit areas shows that there is a strong winnowing action, with the largest particles preferentially deposited. It is this wide variation in particle size in different areas of a stage, plus the wide difference in deposit density, that inhibits a valid calibration.

(c) Particle size. Differences in apparent spot density on the top stage are dependent upon particle size because very large particles have sufficient inertia to overcome the winnowing effect of (b) and impaction efficiency differences of (a). This is very well shown by comparing Figure 3 (a), where the maximum drop size was 12 microns, with Figure 5 (a), a sample taken in identical conditions except that a 20-micron uniform-droplet aerosol was used.

(d) Effect of cone. The Andersen sampler is fitted with a cone over the top stage like an inverted funnel, with an intake hole one inch in diameter. This cone does not spread the aerosol evenly over the top sieve, as perhaps intended, but directs a broad jet of air at the central zone of the sieve. This impacts a high proportion of large particles on the upper surface of the sieve, and those that get through the holes are preferentially impacted in the center. Figure 5 (b) demonstrates this effect in the 20-micron aerosol and should be compared with 5 (a), its parallel sample with no cone. Quantitative estimation of these samples showed that of the drops entering the cone, in (b), 87 per cent were lost on the sieve and 13 per cent recovered from the dish, whereas 78 per cent were recovered from dish (a). These effects get worse, of course, as the particle size increases. At 30 microns only 4 per cent were recovered from the dish when using the cone, compared with 47 per cent without the cone. Even with droplets 12 microns and below, the cone effect is very obvious, as seen by comparing the two parallel Stage 1 samples (a) and (b) in Figure 3.

The above effects are highly reproducible with any kind of particle.

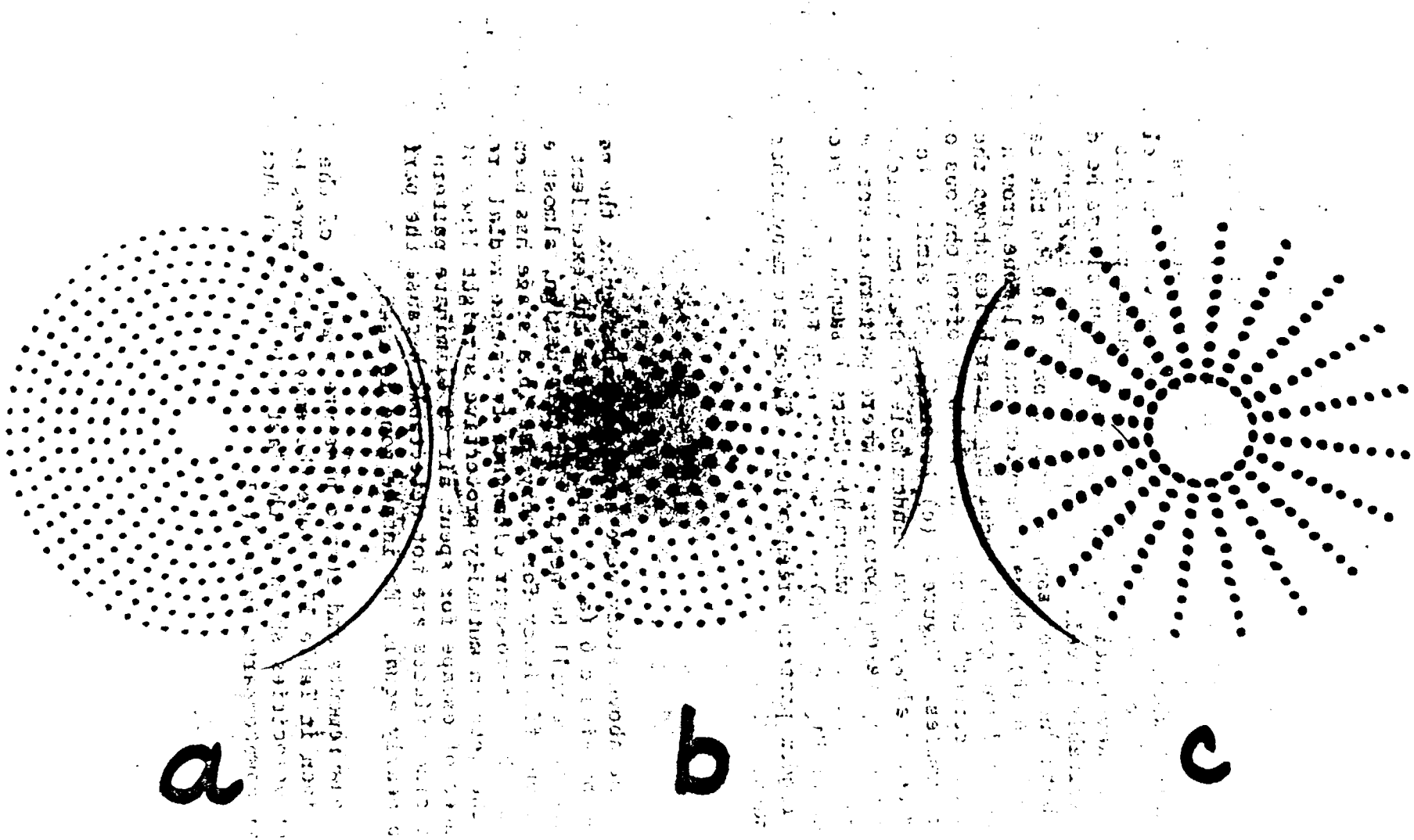

Figure 5. Heavy Samples of Dyed Droplets of 20-Micron Diameter. a, Standard Andersen sampler stage 1 without cone; b, ditto with cone; c, new stage 0, no cone.

A. COLONY PATTERNS

Colonies from a viable aerosol of particle size distribution similar to that in Figure 3 are shown in Figure 4. With colony samples it is not permissible to have an average of more than about three particles per hole, or dishes become overloaded. At this level the Poissonian statistics of the probability of a hole's being occupied blur the effects of factors (a) through (d) above. Also, an occupied hole grows a single colony that has the same apparent "spot density" whether it grows from a single cell particle, a particle containing thousands of cells, or from several mixed particles impacted under the same spot. Nevertheless, pattern effects can always be detected on colony samples of suitable level. Comparing the samples in Figure 3 (a) and 4 (a) we see that both "no cone" samples have a bare area in the central zone. The next colony sample, 4 (b), shows a heavier central zone growth than (a), induced by the cone, and the growth under the outer holes shows the beginnings of preferential "street" deposition, which is often obvious on this stage with heavier samples. Figure 4 (c) is strikingly similar to Figure 3 (c). Stages 3 and below always give random hole occupation, which is as desired. An independently taken photograph where pattern effects may be detected is Andersen's Figure 6,[1] where his Stage 1 sample is directly comparable with the present Figure 4 (b) and Stage 2 with Figure 4 (c). His dishes, of course, have a random pattern orientation. There are many other confirmatory samples at hand.

B. MODIFICATIONS

The lessons of the above study were applied in designing the new radial pattern illustrated by Figure 6 (a, b, and c), where the excellent spot-uniformity over each stage will be noted. In this design, almost equal velocity and impaction efficiency for every jet in a stage has been achieved by (a) adjustment of the jet-to-agar clearance to reduce radial pressure fall, and (b) by having the jets in mutually protective straight lines with clear, and expanding avenues of escape for spent air to eliminate pattern interference. Particle size effects are not detectable because the performance of all holes is so nearly equal. No intake cone is used.

The principal measurements and static pressure readings of the three new radial stages are given in Table II. Note the small differences between the outer and inner jet velocities shown by the last column, which should be compared with their counterparts in Table I.

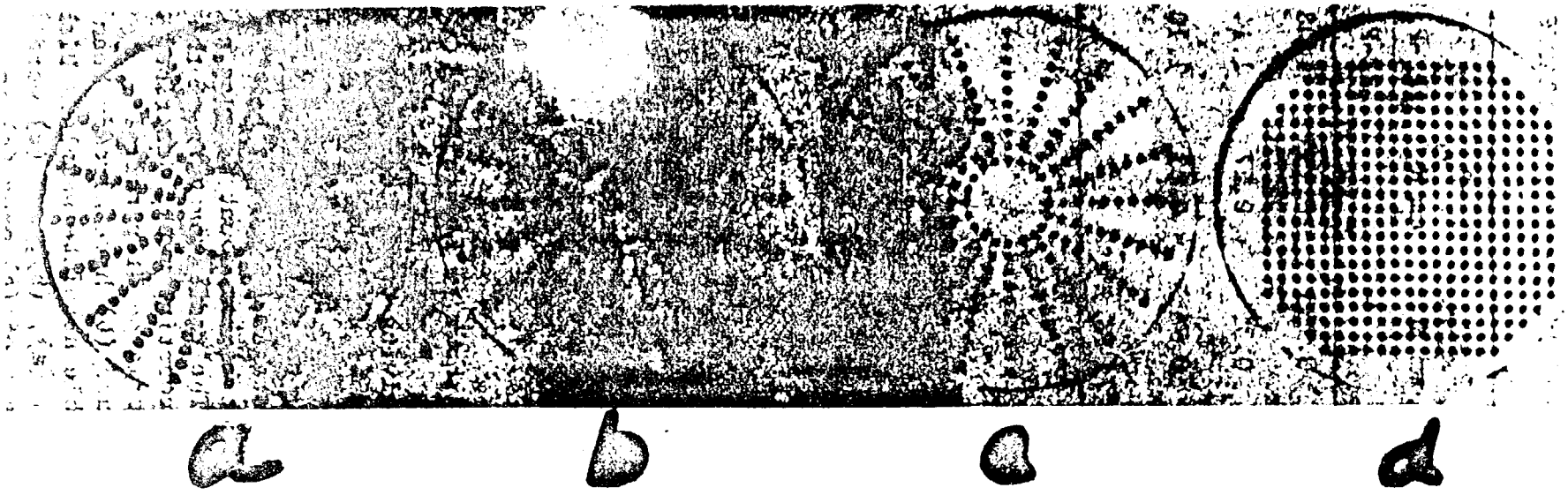

Figure 6. Heavy Sample of Dyed Droplets on Modified Stages. Parallel with Figure 3. a, Stage 0; b, stage 1M; c, stage 2M; d, stage 3M.

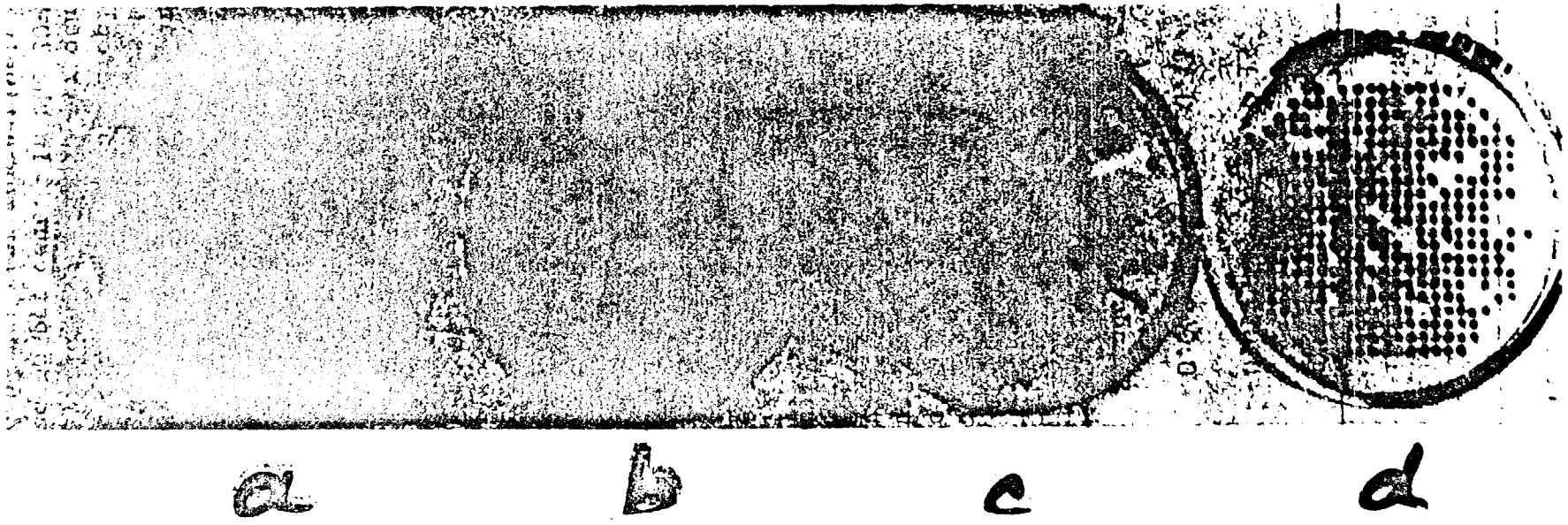

Figure 7. Colonies of S. marcescens from Modified Stages. Parallel sample with Figure 4. a, b, c, and d as for Figure 6.

TABLE II. CHARACTERISTICS OF MODIFIED, 200-HOLE RADIAL PATTERN STAGES

Stage	Hole Diam., inches	Jet-Agar Clearance, inches	P_y-P_z, mm H_2O	P_x-P_z, mm H_2O	P_x-P_y, mm H_2O	$\left(\frac{P_x-P_z}{P_x-P_y}\right)^{\frac{1}{2}}$
0	0.073	0.22	0.022	0.155	0.133	1.08
1M	0.0595	0.15	0.080	0.35	0.27	1.14
2M	0.049	0.11	0.13	0.76	0.63	1.10
3 & below	Standard	0.07	See Table I			

Figure 8 shows the modified radial hole components. In the foreground Stage 1M has been disassembled to indicate the method of pressing a new sieve-plate into the standard Andersen body to obtain the jet-agar clearances of Table II. Jet holes in the radial stages are given a 90-degree countersink to half their depth. Machinists' drawings are available.

Each radial stage has 200 holes in 20 radii. Each radius has 10 holes spaced one-eighth of an inch apart. There is not room for more holes without nullifying the design principle of these stages. Thus we have a total of 600 holes in three top stages compared with 800 in the two top standard Andersen stages. Fewer holes in this five-micron particle range are no disadvantage because, in the general nature of aerosols, large particles are relatively few, so that it is highly unlikely that upper stages will become overloaded before the lower.

Colony growth in the new Stages 0, 1, and 2 is shown in Figure 7 and compares with Figure 4, which is a parallel sample. Figure 7 (a, b, and c) shows 16, 109, and 182 positive holes (total 307) giving corrected counts, from the "positive hole conversion table"[1] modified as described below, of 17, 157, and 482 (total 656). Figure 4 (b and c), show 56 and 185 colonies (total 241), which become on correction 60 and 248 (total 308), although Andersen considers that the counts on his top two stages should not be corrected. In any case, the new stages show a much higher count because of the improved intake and deposition of particles. The radial pattern of the very light sample 7 (a) is not apparent until the counting mask, described later, is used. Figure 5 compares the intake performance of parallel samples in a 20-micron uniform-droplet cloud; (a) and (b) have already been quoted as yielding 78 and 13 per cent of the probable absolute sample. Dish (c) yielded 85 per cent. In the 30-micron aerosol, (a), (b), and (c) were 47, 4, and 67 per cent respectively. The improvement of (c) over (a) is due entirely to having larger holes with a countersunk lead-in. This greatly reduced the particle loss that is observed to occur close to the entrance of the standard parallel holes, because velocity gradients are less.

Figure 8. Modified Stages. Stage 1M disassembled. (FD Neg C-7169)

C. COLONY-COUNTING PROCEDURE

Microscopic examination of the deposits of bacterial particles showed that the effective deposit area of a jet has roughly twice the diameter of the jet. On the new Stage 0 the jet hole diameter is 1.85 mm and individual colonies can therefore usually be counted if they are not larger than about 0.5 mm and are few in number. If they are larger or there is coalescence of colonies as in Figure 7 (b) and (c), "positive holes" should be counted and corrected as described by Andersen.[1] Corrections for the counts from the new 200-hole stages can readily be obtained from Andersen's 400-hole table. If n positive holes are counted, the corrected number for 2n holes is read from the 400-hole table and that number is halved.

Some colonies are found to be out of the hole pattern. These should be ignored, on whatever stage they may be, because they are usually from small particles that have been deposited by the turbulence between jets, on their way to the stages below. The identification of in-pattern colonies on these radial stages is greatly facilitated by the use of the mask shown on the left in Figure 9. Translucent plastic is probably the best mask material. When the mask is correctly oriented in or under the Petri dish, positive or negative holes are instantly recognized by looking through the holes of the mask. On heavy deposits it is quicker to count the few negative holes rather than the many positive ones. The holes are of the same size as for Stage 0. The pattern of the holes is a slight expansion of the Stage 0, 1, and 2 pattern because jets are dragged slightly outwards by the spent air. A drawing is available.

D. NEW HOLE PATTERN FOR THE LOWER STAGES

The success of the counting mask on the radial stages suggested that it would be an advantage to use one for all stages. This cannot be done with the standard unsymmetrical Andersen pattern because there is no way of recognizing the correct orientation for a mask over the colonies. A new pattern must be symmetrical so that the correct mask position is unequivocal. To give maximum utilization of the agar surface in the lower stages, at least 400 holes are required, but because holes should not be closer than one-eighth inch, a 400-hole radial pattern would give overcrowding. Also, a radial pattern is no longer necessary for the lower stages, where jet velocities are sufficiently equal and high to give an even deposit pattern. The rectangular pattern of 400 holes with one-eighth inch spacing as shown in Figure 6 (d) was therefore adopted. Hole sizes and other dimensions are exactly the same as for the standard Stages 3 through 6. The mask is shown on the right of Figure 9, and again it is a slight expansion of the hole pattern.

Figure 9. Counting Masks for Radial and Rectangular Hole Patterns. (FD Neg C-7170)

This system is very successful in giving a rapid count of positive or negative holes, whichever is the fewer, and in eliminating out-of-pattern colonies. Even without the mask, the colonies of Figure 7 (d) are obviously easier to count than the exact counterpart, Figure 4 (d). The greatest advantage of the rectangular pattern is perhaps in its facilitation of microscopic counting of inert particle deposits.

E. CALIBRATION

The cut-off curves for unit density spheres are shown in Figure 2. They are strikingly similar to those calculated from the experimental results of Ranz and Wong,[4] which were obtained from a single-jet system of rather similar geometry and are shown as dashed lines. The true curve for Stage 6, which cannot be obtained from the present work, is therefore probably similar to the dashed curve for that stage.

Stages 0 and 1M have rather long "tails" because of the retention of a small number of particles down to three or four microns. This defect is inherent in the system, and could cause a spurious apparent count of large particles in aerosols having great numbers of small viable particles with very few large ones. Such error can be avoided by taking a parallel impactor sample for measurement of the largest particles by microscope, a procedure that must be done in any case to draw complete size-distribution curves.

The size range of unit density spheres on each stage except for Stage 0, which has no upper limit, can be obtained from Figure 2. Thus, Stage 3 begins to receive particles of about 4.5 microns from Stage 2 and slips all particles smaller than 2.1 microns. For particles of other density, ρ, all diameters should be divided by $\sqrt{\rho}$. The mass-distribution curves for each stage are given in Figure 10. Except for the Stage 0 curve, these are nearly constant for each stage where the aerosol has sufficient size range to cover them fully. The Stage 0 curve applies only to one particular aerosol, because it has no fixed upper limit.

The principal parameters derived from the calibration are in Table III, which is used as follows. From corrected bacterial colony counts, the number distribution curve can be drawn by plotting the d_{50} values for the appropriate particle density against the cumulative numbers on the stages below. The mass-distribution curve can be obtained from this in the conventional way. Volume on each stage is the product of the colony count and the volume obtained from the mean volume diameter, where the aerosol size range adequately covers the stage. This figure can be used to estimate total cells per stage from samples of sprayed suspensions when the total solids content and cell count of the suspension are known, and when there has been no viable decay. A comparison with impinger samples can therefore be made. Good agreement has been obtained in several of such tests.

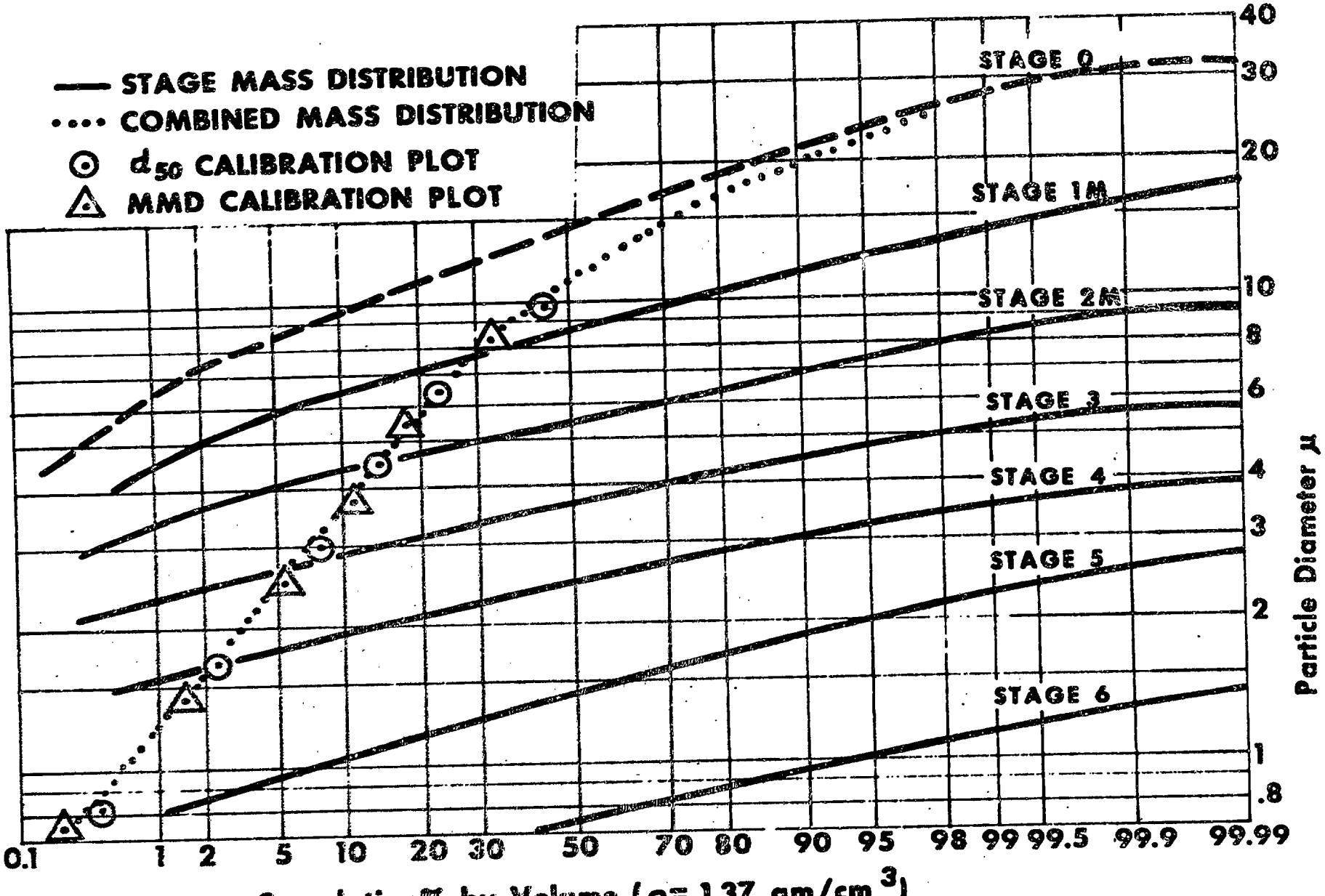

Figure 10. Volume Distribution Curves of Modified Andersen Sampler from a Sprayed Bacterial Aerosol.

TABLE III. CALIBRATION OF MODIFIED ANDERSEN SAMPLER FOR UNIT DENSITY SPHERES AND FOR TYPICAL BACTERIAL PARTICLES

Stage	AT DENSITY 1 gm/cm^3			AT DENSITY 1.37 gm/cm^3		
	d_{50}, μ	Mass Median Diameter, μ	Mean Volume Diameter, μ	d_{50}, μ	Mass Median Diameter, μ	Mean Volume Diameter, μ
0	11.2			9.5		
1M	7.5	10	8.3	6.5	8.5	7.0
2M	5.4	6.6	6.2	4.6	5.6	5.3
3	3.5	4.4	4.2	3.0	3.7	3.5
4	2.0	3.0	2.7	1.7	2.5	2.3
5	0.97	1.5	1.4	0.83	1.4	1.2
6	0.6[a]	0.9	0.85	0.5[a]	0.77	0.73

a. Calculated from Ranz and Wong.[4]

With nonviable samples that can be estimated, say, chemically, mass-distribution curves can be plotted directly from the stage estimates and the d_{50} values. Alternatively, the MMD's of Table III can be plotted against the cumulative mass for the stages below plus half that on the stage. The circles and triangles in Figure 10 compare these methods of plotting with the dotted curve, which is from the summed counts of the aerosol that gave the Stage 0 curve.

IV. DISCUSSION

Stages 3 and below in the Andersen Sampler (model 0101) function in a very satisfactory manner and in accord with the previous work of Ranz and Wong.[4] There is almost no slippage of particles beyond their proper stage. Stages 1 and 2 are not satisfactory and the modifications described and the calibration given enable most of the important aerosol parameters to be obtained from the colony counts. The sampler has other desirable features, such as simplicity and speed in use, and is rugged.

It is recommended that workers with modified forms of any stage should test them for jet uniformity by the heavy sample method, sprayed clouds of india ink sampled on milk-agar being particularly suitable. Also, the intake cone should be discarded where possible because of the heavy loss of larger particles it causes on the top sieve.

Attempts to extend the size discrimination further upward beyond the present work meet with the difficulty of high internal loss because large particles are unable to make the 360-degree turn to the next stage. All detectable wall loss in the Andersen Sampler is found on the sieves near the jet entrances and on the internal dish walls just above the agar. In the present geometry these losses are unimportant.

When sampling in a wind, the sampler should be laid on its side facing into the wind. One may speculate that the broad multi-hole suction area may be a reasonable alternative, at least up to 20 microns, to isokinetic sampling, which in any case cannot be usefully achieved in a natural wind.

The use of the Andersen Sampler is of course by no means confined to bacterial aerosols. Its high stage capacity will often be very useful for obtaining bulk samples of any kind of air-borne dust or fine spray. For microscopy, the deposition of the sample in a large number of small, equal spots, each of which can be scanned in a few fields, is particularly useful. The impaction of particles is very gentle and there is absolutely no risk of particle or droplet shatter.

LITERATURE CITED

1. Andersen, A.A. "New sampler for the collection, sizing and enumeration of viable air-borne particles," J. Bacteriol. 76:471-484, 1958.

2. Mercer, T.T. "On the calibration of cascade impactors," Ann. Occup. Hyg. 6:1-14, 1963.

3. May, K.R. "The cascade impactor: an instrument for sampling coarse aerosols," J. Sci. Instr. 22:187-195, 1945.

4. Ranz, W.E., and Wong, J.B. "Jet impactors for determining the particle size distribution of aerosols," A.M.A. Arch. Indust. Hyg. and Occupational Med. 5:464-477, 1952.